Karpen J.W., Zimmerman A.L., Stryer L. & Baylor D.A. (1988) *Proc. Natl. Acad. Sci. USA* **85**, 1287–1291.
Klodos I. & Forbush B. III (1988) *J. Gen. Physiol.* **92**, 46a (abstract).
Komori S. & Bolton T.B. (1991) *Pflügers Arch.* **418**, 437–441.
Korth M. & Engels J. (1979) *Naunyn-Schmiedeberg's Arch. Pharmacol.* **310**, 103–111.
Lando L. & Zucker R.S. (1988) *J. Gen. Physiol.* **93**, 1017–1060.
Lester H.A. & Chang H.W. (1977) *Nature* **266**, 373–374.
Lester H.A. & Nerbonne J.M. (1982) *Ann. Rev. Biophys. Bioengng* **11**, 151–175.
Lester H.A., Chabala L.D., Gurney A.M. & Sheridan R.E. (1986) In *Optical Methods in Cell Physiology (Soc. Gen. Physiol. Ser.)*, P. De Weer & B. Salzberg (eds). Wiley, New York, pp. 447–462.
McCray J.A. & Trentham D.R. (1989) *Ann. Rev. Biophys. Chem.* **18**, 239–270.
McCray J.A., Herbette L., Kihara T. & Trentham D.R. (1980) *Proc. Natl. Acad. Sci. USA* **77**, 7237–7241.
Matsunaga K. & Furchgott R.F. (1989) *J. Pharmac. Exp. Ther.* **248**, 687–695.
Messenger J.B., Katayama Y., Ogden D.C., Corrie J.E.T. & Trentham D.R. (1991) *J. Physiol.* **438**, 293P.
Milburn T., Matsubara N., Billington A.P., Udgaonkar J.B., Walker J.W., Carpenter B.K., Webb W.W., Marque J., Denk W., McCray J.A. & Hess G.P. (1989) *Biochemistry* **28**, 49–55.
Moncada S., Palmer R.M.J. & Higgs E.A. (1991) *Pharmacol. Rev.* **43**, 109–142.
Nargeot J., Lester H.A., Birdsall N.J.M., Stockton J., Wassermann N.H. & Erlanger B.F. (1982) *J. Gen. Physiol.* **79**, 657–678.
Nargeot J., Nerbonne J.M., Engels J. & Lester H.A. (1983) *Proc. Natl. Acad. Sci. USA* **80**, 2395–2399.
Naebauer M., Ellis-Davies G.C.R., Kaplan J.H. & Morad M. (1989) *Am. J. Physiol.* **256**, H916–H920.
Nerbonne J.M. (1986) In *Optical Methods in Cell Physiology (Soc. Gen. Physiol. Ser.)*, P. De Weer & B. Salzberg (eds). Wiley, New York, pp. 417–445.
Nerbonne J.M. & Gurney A.M. (1987) *J. Neurosci.* **7**, 882–893.
Nerbonne J.M., Lester H.A. & Connor J.A. (1982) *Soc. Neurosci. Abstr.* **8**, 945a.
Nerbonne J.M., Sheridan R.E., Chabala L.D. & Lester H.A. (1983) *Molec. Pharmacol.* **23**, 344–349.
Nerbonne J.M., Richard S., Nargeot J. & Lester H.A. (1984) *Nature* **310**, 74–76.
Nerbonne J.M., Richard S. & Nargeot J. (1985) *J. Molec. Cell. Cardiol.* **17**, 511–515.
Nichols C.G., Niggli E. & Lederer W.J. (1990) *Pflügers Arch.* **415**, 510–512.
Ogden D.C., Capiod T., Walker J.W. & Trentham D.R. (1990) *J. Physiol.* **422**, 585–602.
Patchornik A., Amit B. & Woodward R.B. (1970) *J. Am. Chem. Soc.* **92**, 6333–6335.
Richard S., Nerbonne J.M., Nargeot J., Lester H.A. & Garnier D. (1985) *Pflügers Arch.* **403**, 312–317.
Sheridan R.E. & Lester H.A. (1982) *J. Gen. Physiol.* **80**, 499–515.
Shimada K. & Berg H.C. (1987) *J. Molec. Biol.* **193**, 585–589.
Shinkai S., Matsuo K., Harada A. & Manabe O. (1982) *J. Chem. Soc. Perkin Trans.* **2**, 1261–1265.
Somlyo A.P. & Somlyo A.V. (1990) *Ann. Rev. Physiol.* **52**, 857–874.
Somlyo A.P. Walker J.W., Goldman Y.E., Trentham D.R., Kobayashi S., Kitazawa T. & Somlyo A.V. (1988) *Phil. Trans. R. Soc. Lond. B* **320**, 399–414.
Spray D.C., Nerbonne J.M., Campos De Carvalho A., Harris A.L. & Bennet M.V.L. (1984) *J. Cell Biol.* **99**, 174–179.
Tsien R.Y. (1980) *Biochemistry* **19**, 2396–2404.
Tsien R.Y. & Zucker R.S. (1985) *Biophys. J.* **50**, 843–853.
Valdeolmillos M., O'Neill S.C., Smith G.L. & Eisner D.A. (1989) *Pflügers Arch.* **413**, 676–678.
Walker J.W. (1991) In *Cellular Neurobiology: A Practical Approach* J. Chad & H. Wheal (eds). IRL Press at Oxford University Press, Oxford. pp. 179–203.
Walker J.W. & Trentham D.R. (1988) *Biophys. J.* **53**, 596a.
Walker J.W., McCray J.A. & Hess G.P. (1986) *Biochemistry* **25**, 1799–1805.
Walker J.W., Somlyo A.V., Goldman Y.E., Somlyo A.P. & Trentham D.R. (1987) *Nature* **327**, 249–252.
Walker J.W., Reid G.P., McCray J.A. & Trentham D.R. (1988) *J. Am. Chem. Soc.* **110**, 7170–7177.
Walker J.W., Reid G.P. & Trentham D.R. (1989a) *Methods Enzymol.* **172**, 288–301.
Walker J.W., Feeney J. & Trentham D.R. (1989b) *Biochemistry* **28**, 3272–3280.
Wigilius I.M., Axelsson K.L., Andersson R.G.G., Karlsson J.O.G. & Odman S. (1990) *Biochem. Biophys. Res. Commun.* **169**, 129–135.
Wolin M.S., Omar H.A., Mortelliti M.P. & Cherry P.D. (1991) *Am. J. Physiol.* **261**, H1141–H1147.
Wootton J.F. & Trentham D.R. (1989) In *Photochemical Probes in Biochemistry*, P.E. Nielsen (ed.). NATO ASI series C, Vol. 272. Kluwer, Dordrecht, pp. 277–296.
Zucker R.S. & Hayden P.G. (1988) *Nature* **335**, 360–362.

CHAPTER FORTY-ONE

Fluorescent Analogues: Optical Biosensors of the Chemical and Molecular Dynamics of Macromolecules in Living Cells

K. HAHN, J. KOLEGA, J. MONTIBELLER, R. DeBIASIO, P. POST, J. MYERS & D.L. TAYLOR
Center for Light Microscope Imaging and Biotechnology, Carnegie Mellon University, Pittsburgh, PA, USA

41.1 INTRODUCTION

Fluorescent analogue cytochemistry has grown to produce important insights in a wide variety of fields since 1978, when it was first demonstrated that a protein labelled with a fluorescent dye could function and be investigated within living cells (Taylor & Wang, 1978). The fluorescein-actin used in the first experiments exemplified an approach to analogue production which has been used in the large majority of studies to date. Almost all analogues have been made with dyes whose fluorescence is minimally affected by the intracellular environment, thus focusing on analysis of the analogue's distribution within live cells. Meaningful information has been obtained through adherence to several important principles (Taylor & Wang, 1980; Taylor *et al.*, 1984; Simon & Taylor, 1986; Wang, 1989). Chief among these has been careful *in vitro* characterization of the labelled protein prior to interpretation of live cell data (Wang & Taylor, 1980). Minimal perturbation of the analogues' biological function has been sought during labelling, and the effects of dye attachment have been carefully determined. Furthermore, the smallest possible quantity of analogue has been injected to avoid alteration of normal cell function.

Environmentally insensitive fluorescent analogues of many different proteins have been successfully observed in live cells. Examples include analogues of actin-binding proteins (myoin, vinculin, *a*-actinin), which have revealed complex changes in the cytoskeleton during a number of physiological processes (Wang *et al.*, 1982; Kreis & Birchmeier, 1982; Simon & Taylor, 1986; Kolega & Taylor, 1991). Labelled tubulin has shown the location and extent of tubulin exchange in the mitotic spindle, thus testing different models of spindle function (Salmon *et al.*, 1984; Wadsworth & Salmon, 1986; Gorbsky *et al.*, 1987). Calmodulin analogues have revealed the changing distribution of calmodulin during mitosis, and indicated transient calmodulin association with various

FLUORESCENT AND LUMINESCENT PROBES, 2ND EDN
ISBN 0–12–447836–0

subcellular organelles (Zavortink *et al.*, 1983; Luby-Phelps *et al.*, 1985). A recent addition to this family of probes have been protein analogues labelled with 'caged' fluorophores, whose fluorescence is activated by irradiation (Ware *et al.*, 1986; Mitchison, 1989; Theriot & Mitchison, 1991). This approach has permitted the marking of a subpopulation of analogues for temporal-spatial tracing at high contrast (Mitchison, 1989; Theriot & Mitchison, 1991).

More recently, the first representatives of a new family of fluorescent protein analogues have been developed using environmentally sensitive fluorophores, as proposed earlier (Taylor & Wang, 1980). These analogues have served as indicators of protein activity, in that the attached dye reflected conformational changes or altered ligand binding by the proteins. An environmentally sensitive dye has been used to make an analogue of calmodulin whose fluorescence reflects calcium-calmodulin binding (Hahn *et al.*, 1990). This analogue has been used in conjunction with a fluorescent calcium indicator to correlate the spatial and temporal dynamics of calcium transients and calium-calmodulin binding in individual, living cells. Details of these studies are described below. Resonance energy transfer between two fluorophores has been applied in an alternate approach to fluorescent sensing of protein activity. Energy transfer is strongly affected by protein changes that alter the distance between donor and acceptor dyes. The approach has been used to monitor actin polymerization *in vitro* (Taylor *et al.*, 1981; Wang & Taylor, 1981). When mixed fluorescein-actin and rhodamine-actin monomers were brought in proximity during polymerization energy transfer increased dramatically. More recently, the catalytic and regulatory subunits of protein kinase A have been labelled with fluorescein and rhodamine (Adams *et al.*, 1991). Dissociation of the subunits by cAMP was observed in live cells as a decrease in energy transfer.

In our laboratory, we are harnessing environmentally sensitive and insensitive protein analogues to decipher the mechanics and regulation of cell motility. We will describe here our efforts to use fluorescent analogue cytochemistry in elucidating the mechanisms by which extracellular stimuli induce cell contraction and initiation of motility. Our aim is to define the often rapid changes in second messengers involved in this process, and their effects on the dynamics of contractile proteins in time and space during cell function.

In the currently established paradigm of stimulus-contraction coupling in non-muscle cells (for reviews see McNeil & Taylor, 1987; Sellers & Adelstein, 1987), binding of ligands to external receptors leads to intracellular production of lipid metabolites and alterations in the concentration and distribution of calcium. We are initially focusing on subsequent regulatory steps involving modulation of the calcium signal through calmodulin and myosin light chain kinase. Calcium binding to calmodulin enables calmodulin to activate myosin light chain kinase, which phosphorylates myosin II regulatory light chains. This phosphorylation activates myosin for contraction.

We will describe protein-based fluorescent indicators (optical biosensors) for observation of individual signalling steps in this process. The production and application of fluorescent analogues used as biosensors of calcium-calmodulin binding will be described, as will progress towards indicators of myosin light chain phosphorylation. The use of fluorescent analogues of actin and myosin to study the dynamics of contractility will also be described.

We study serum stimulation of quiescent fibroblasts (McNeil & Taylor, 1987) and a 'wound healing' model in which a gap is introduced in a monolayer of fibroblasts using a blunt razor blade (DeBiasio *et al.*, 1988; Fisher *et al.*, 1988). Fibroblasts at the edge of this 'wound' migrate into the gap. In these systems, the timing of stimulation can be controlled, and during wound healing, polarized movement occurs with a predetermined orientation. Cells are observed with a multimode microscope imaging system that permits rapid switching between transmitted light microscopy and various forms of fluorescence microscopy using different detectors and excitation and emission filters (Giuliano *et al.*, 1990).

41.2 MEROCAM 1 AND 2: FLUORESCENT INDICATORS OF CALCIUM–CALMODULIN BINDING

Fluorescent calcium indicators have been invaluable in elucidating the kinetics and intracellular distribution of calcium transients during a wide range of cellular processes (Tsien, 1989). However, subsequent signalling steps have to date remained inaccessible to observation *in vivo*. We have designed a fluorescent indicator of calcium–calmodulin binding which we are now using to correlate intracellular calcium changes with calmodulin activation during growth factor stimulation of quiescent fibroblasts (Hahn *et al.*, 1990). We are correlating the spatial and temporal dynamics of calcium changes and calcium–calmodulin binding. Biochemical evidence indicates that calmodulin's calcium response will depend on its intracellular environment. Calmodulin's calcium affinity is affected by target proteins (Cohen & Klee, 1988), and calmodulin binds to different targets at different calcium levels (Andreason *et al.*, 1983; Cohen & Klee,

1988). Changing subcellular distribution of calmodulin seen in previous studies using environmentally insensitive fluorescent analogues supports regulation of calmodulin by factors in addition to calcium (Pardue *et al.*, 1981; Zavortink *et al.*, 1983; Luby-Phelps *et al.*, 1985).

We have designed our indicators of calcium–calmodulin binding on the basis of previous biochemical studies which show that calmodulin–calcium binding produces a hydrophobic site on calmodulin with affinity for specific small molecules (LaPorte *et al.*, 1980, 1981; Malencik *et al.*, 1981; Manalan & Klee, 1984; Cohen & Klee, 1988). Structure–activity studies enabled synthesis of a novel dye with both highly solvent-sensitive fluorescence and strong affinity for calmodulin's calcium-induced hydrophobic binding site. Through affinity labelling, this dye was covalently attached to calmodulin in a position where it would have access to the calcium-induced hydrophobic pocket. Whenever calcium bound calmodulin, the solvent-sensitive dye moved into the hydrophobic pocket, with a consequent shift in fluorescence. The fluorescence change was shown to be fully reversible on removal of calcium. We named the calcium–calmodulin binding indicator meroCaM 1, for merocyanine dye + calmodulin.

Spectral characterization of meroCaM 1 showed that its excitation spectrum changed in both intensity and peak shape in a calium-dependent manner. The spectral changes were suitable for ratio imaging, an important technique used to normalize fluorescence of analogues in the cell for differences in cell thickness, excitation intensity, and other factors (Tanasugarn *et al.*, 1984; Bright *et al.*, 1989). The excitation ratio varied sigmoidally with calcium, and showed an overall 3.4-fold change. Unlike other solvent-sensitive fluorophores, the dye used in meroCaM 1 was designed specifically for use in live cells. Optimum excitation ratios were obtained at 532 and 608 nm (emission 623 nm), long wavelengths which do not cause photodamage of cells and are far from the autofluorescence of mammalian cells. The dyes had high absorbance and quantum yield values, decreasing the amount of intracellular protein analogue required to obtain acceptable fluorescence signal.

In order to apply meroCaM 1 to study regulation of calmodulin activity, it was important to characterize the analogue's target protein binding, and to show that the effects of target proteins on calcium affinity remained intact. MeroCaM 1 was shown to retain calmodulin's ability to activate myosin light chain kinase, a calmodulin target protein. It also showed calcium-dependent mobility on native and SDS gels. Known effects of melittin and cAMP-phosphodiesterase on calcium affinity were also observed in meroCaM 1.

The calcium-induced change in meroCaM 1 fluorescence was half maximal at 0.3–0.4 μM, below the 5–10 μM apparent dissociation constant reported for overall calcium–calmodulin binding (Klee, 1988). This could have resulted from the dye stabilizing calmodulin's calcium-bound form, thus affecting the calcium binding constant. Alternately, the dye could have been positioned on the protein where it would reflect primarily binding to the high-affinity calcium sites. These possibilities were distinguished by comparing the calcium dependence of meroCaM 1 and calmodulin cAMP-phosphodiesterase activation. The similar behaviour of the two proteins in this assay indicated that meroCaM 1 fluorescence reflected binding to high-affinity calcium sites. The effect of cAMP-phosphodiesterase binding on calmodulin's calcium affinity remained intact in meroCaM. The assay did show that meroCaM's maximal activation or affinity for the phosphodiesterase was somewhat reduced from that of calmodulin.

In order to assay the effect of target protein binding on meroCaM 1 fluorescence, the calcium dependence of the excitation ratio was determined in the presence and absence of melittin, a peptide mimic of target proteins' calmodulin binding sites (Comte *et al.*, 1983; Maulet & Cox, 1983; Cox *et al.*, 1985; Seeholzer *et al.*, 1986). These experiments showed that the high and low excitation ratio values, produced at extremes of calcium concentration, were altered by melittin. Although this will complicate quantitation of the extent of calcium-calmodulin binding, quantitative analysis of binding kinetics should not be affected.

We have begun testing meroCaM 1 in live cells. The analogue has shown sufficient brightness and photostability to obtain greater than 10 ratio pairs, and has shown no apparent toxic effects or alteration of cell physiology. In our preliminary studies, meroCaM 1 has been injected in Swiss 3T3 fibroblasts made quiescent by 48 h incubation in low serum medium. Published studies and our own work have shown that these cells respond to whole serum with a rapid and transient upsurge in intracellular calcium (Byron & Villereal, 1989; Tucker & Fay, 1990; Takuwa *et al.*, 1991; McNeil *et al.*, 1985; Taylor, DeBiaiso & Hahn, (pers. commun.)). When the cells containing meroCaM 1 were challenged with whole serum, the intracellular meroCaM 1 excitation ratio increased 10–15% within 1 min and then returned to baseline over a period of several minutes. The filters used to excite and monitor the analogue's fluorescence have not been optimized, so it is anticipated that greater fluorescence responses will ultimately be obtained. Mapping of meroCaM 1 response within individual cells indicated spatial heterogeneity of calmodulin activation.

We have also developed new dyes in an effort to

improve meroCaM 1, and have found that substitution of a benzoxazole moiety for benzothiazole in the meroCaM 1 dye results in a strong enhancement of fluorescence response. The new dye has been attached to calmodulin to produce a protein analogue which we call meroCaM 2. The excitation ratio of this indicator shows a 7-fold calcium-dependent change in excitation ratio (excitation 457, 569 nm; emission 587 nm). In preliminary studies, the indicator has been injected in quiescent Swiss 3T3 fibroblasts together with the fluorescent calcium indicator, Calcium Green (Plate 41.1) (Molecular Probes, Eugene, OR). Stimulation of the cells with whole serum caused a rapid increase in calcium to maximal levels within 1 min, followed by a decrease which sometimes showed smaller additional maxima. The response of MeroCaM 2 to these calcium changes was quite complex. MeroCaM response generally also reached its maximum (up to 80% increase) within the first minute after stimulation, but afterwards sometimes paralleled calcium changes and sometimes underwent independent oscillations.

The correlation of calcium–calmodulin binding with calcium changes in living cells now appears to be within reach. We hope to extend the approach we have developed to produce indicators of calmodulin binding to target proteins. Published studies indicate that sensitivity of fluorescent calmodulin derivatives to calcium vs. protein binding is strongly dependent on dye structure and the position of dye attachment (LaPorte *et al.*, 1981; Mills *et al.*, 1988). We will test new dyes and explore the use of site-specific mutagenesis to introduce cysteines for attachment of dye at precise positions.

41.3 FLUORESCENT ANALOGUE OF MYOSIN II

The simplest form of fluorescent analogue is one whose fluorescence is insensitive to configuration and local environment. Such analogues act as direct reporters of a molecule's distribution and movements. A variety of clever biophysical and optical techniques have been used to parlay this simple information into local chemical concentrations, state of molecular assembly, diffusion constants, and a number of other detailed analyses of molecular dynamics at a subcellular level. As an example of some of these applications, we will discuss fluorescent analogues of myosin II that have been produced to visualize directly the dynamics of myosin II during cell movement in single, living Swiss 3T3 fibroblasts.

Smooth muscle myosin II isolated from chicken gizzard was labelled with tetramethyl rhodamine iodoacetamide (DeBiasio *et al.*, 1988). The dye was covalently bound to both the myosin II heavy chain and the 17 kDa light chain, leading to incorporation of 4–6 mol dye per mol protein. Before performing *in vivo* studies, it was essential to establish the biological activity of the analogue through careful biochemical characterization. The analogue was shown to retain native myosin II's ability to assemble into filaments as measured by right-angle light scattering (Fig. 41.1), and both labelled and unlabelled filaments were depolymerized by 5 mM ATP. Fluorescent labelling did not affect the analogue's K-EDTA ATPase activity. Labelled and native myosin II were phosphorylated to the same extent and at the same rate by chicken gizzard myosin light chain kinase (Fig. 41.2).

The positions of dye attachment on the heavy chain were determined using the papain digestion procedure of Nath *et al.*, (1986). One fluorophore was located in the 70 kDa *N*-terminal portion of myosin II's S1 region, and another in the S2 region. No fluorophore was detected in the 25 kDa *C*-terminal portion of the S1 head. Modification at the latter site has been shown to cause elevation of actin-activated MgATPase activity in unphosphorylated myo-

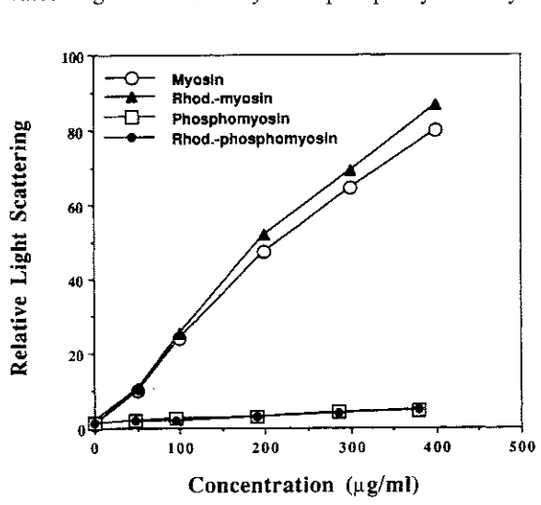

Figure 41.1 Myosin II and rhodamine-myosin II polymerization. The abilities of myosin II and its rhodamine analogue to polymerize were measured by right-angle light scattering using the procedure of McKenna *et al.* (1989). Unlabelled myosin and rhodamine-myosin II were dialysed into 500 mM KCl, 0.1 mM EDTA, 0.1 mM EGTA, 10 mM HEPES, pH 7.5. Dialysates were clarified by centrifugation and the concentrations measured spectrophotometrically using an extinction coefficient of E280 = 0.53 cm^{-1} (0.1%), correcting for 280 nm absorbance due to dye in the case of rhodamine-myosin II. The myosins were diluted 12-fold into an assembly buffer containing 150 mM KCl, 10 mM $MgCl_2$, 1 mM EGTA, 0.1 mM DTT, 10 mM HEPES, pH 7.5 at room temperature. Scattered light intensities were measured at 340 nm using a Perkin-Elmer MPF-3 fluorescence spectrophotometer. To test the sensitivity of the filaments to ATP, the assembly mixtures were made 5 mM in ATP and the measurements were repeated.

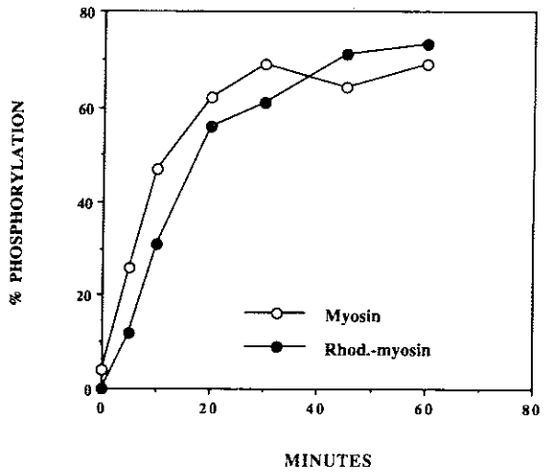

Figure 41.2 Phosphorylation of myosin II and rhodamine-myosin II. Myosin II or rhodamine-myosin II (c. 4 mg ml^{-1}) were phosphorylated at room temperature in a mixture containing 25 mM Tris-HCl, 4 mM $MgCl_2$, 1 mM ATP, 15 μg ml^{-1} bovine brain calmodulin, and $CaCl_2$ 0.2 mM in excess of EGTA, pH 7.5. The reaction was started by the addition of 0.6 μg ml^{-1} smooth muscle MLCK in 1 mg ml^{-1} BSA in Tris. Aliquots of 20 μl were removed at intervals, and the reaction was terminated by dilution. Samples were run on glycerol-urea polyacrylamide gels (Perrie & Perry, 1970). The phosphorylated and dephosphorylated 20 kDa light chain bands were stained with Coomassie blue dye and the relative amounts of each were quantified by densitometry. The rate of phosphorylation was slightly higher for the unlabelled myosin, but this was due to the presence of endogenous kinase which had been eliminated from the rhodamine-myosin II during postlabelling purification.

sin II, and to hinder myosin II's ability to adopt a folded conformation (Chandra *et al.*, 1985). A gel filtration assay (Trybus *et al.*, 1982) indicated that folding was unaffected by labelling (Fig. 41.3). Actin-activated MgATPase activity was decreased by 0–40% (Table 41.1). In the absence of actin, the labelling had no effect on this activity.

After biochemical characterization, the analogue was injected into living Swiss 3T3 fibroblasts (DeBiasio *et al.*, 1988), where it permitted direct visualization of myosin II dynamics. Fluorescent myosin II became distributed throughout the cell within 1 h after injection, incorporating into the same structures and displaying the same periodic, 'pseudosarcomeric' distribution revealed by immunofluorescence staining of endogenous myosin II (Fig. 41.4) (DeBiasio *et al.*, 1988; McKenna *et al.*, 1989). Unlike immunofluorescence experiments, use of the analogue permitted observation of myosin II dynamics over extended periods of time, and time-lapse studies revealed that myosin II was very dynamic. In fibroblasts made quiescent by serum deprivation, myosin II assembled into stress fibres at the cell margins, moved centripetally toward the nucleus, and then disassembled in the perinuclear region, presumably recycling to reassemble at the periphery (Giuliano & Taylor, 1990). The intracellular movements of myosin II have also been examined during amoeboid locomotion of endothelial cells (Kolega, 1997) and during cytokinesis (Sanger *et al.*, 1989; DeBiasio *et al.*, 1996) using similar microinjected fluorescent analogues. Furthermore, by preparing fluorescent analogues using myosin II from different tissues, it is possible to generate isoform-specific analogues (Kolega, 1998). When these analogues are labelled with spectrally distinct fluorophores, the dynamic behaviour of different myosin II isoforms can be monitored simultaneously within the same cell.

Dynamic imaging of fluorescent analogues of myosin II has helped elucidate the nature of actin–myosin contractility in living cells. Stimulation of fibroblasts by serum or growth factors causes shortening of stress fibres with concomitant shortening of the pseudosarcomeric spacing (Giuliano & Taylor, 1990). These observations supported a sliding filament model of fibre shortening, as did quantitative analysis of the fibre shortening induced by cytochalasin, an actin-solating agent (Kolega *et al.*, 1991). The amount of fluorescence associated with stress fibres during cytochalasin-induced shortening was measured by integrating the intensity of digital images. The density of the analogue along fibres increased as the fibres shortened, indicating that myosin II became more concentrated during shortening. The *total* analogue associated with the fibre *decreased* during shortening, indicating a significant loss of myosin II from the shortening fibre. This partial 'self-destruct' process is an important component of the solation–contraction coupling hypothesis (Taylor & Fechheimer, 1982; Kolega *et al.*, 1991). Thus, the use of a myosin II fluorescent analogue enabled demonstration of a basic mechanism of cell contractility *in vivo*.

The ability to follow myosin II dynamics in living cells has also illuminated how contractile structures are regulated and distributed in the cytoplasm. It has been shown *in vitro* and in extracted cell models that myosin II assembly and motor activity can be regulated by phosphorylation of myosin II's 20 kDa regulatory light chain (Sellers & Adelstein, 1987; Lamb *et al.*, 1988). Fluorescent analogues of myosin II revealed changes in myosin II organization *in vivo* when light-chain phosphorylation was increased or decreased by inhibitors of intracellular phosphatases and kinases. When serum-deprived 3T3 fibroblasts were treated with okadaic acid, a phosphatase inhibitor, stress fibres contracted slowly, but incompletely (Fig. 41.5). In contrast, staurosporine, a kinase inhibitor, caused dissolution of fibres without shortening (Fig. 41.6). The dissolution of fibres could be quantified using the fluorescence images of the myosin

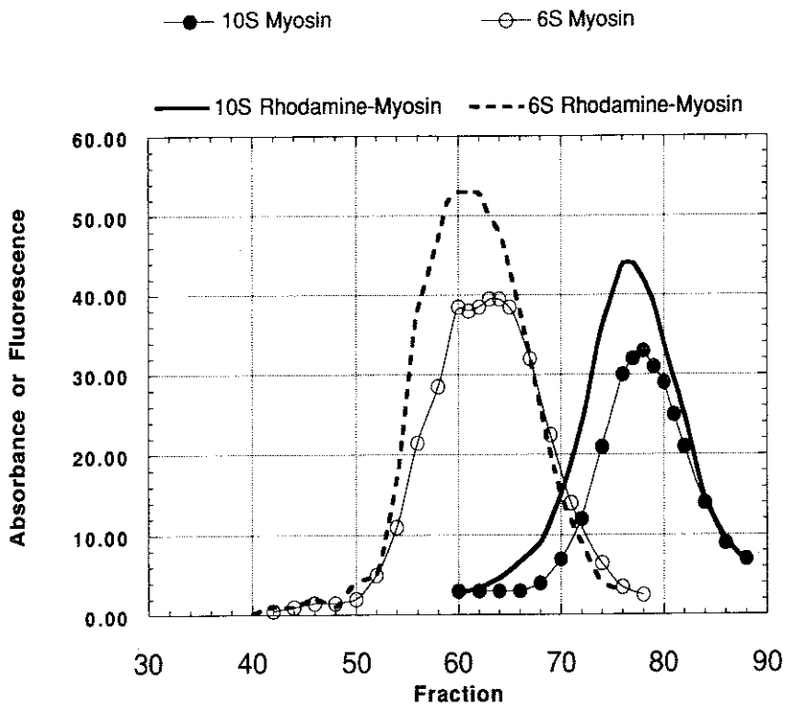

Figure 41.3 Chromatographic assay of ionic strength-dependent myosin II and rhodamine-myosin II conformational change. A 1.5 × 90 cm Sepharose CL-4B column was equilibrated in low salt buffer (150 mM KCl, 5 mM $MgCl_2$, 1 mM EGTA, 10 mM K_nPO4, 1 mM MgATP, pH 7.5) at a flow rate of 6 ml h^{-1} maintained using a peristaltic pump. The column was calibrated with proteins IgG, IgM, and BSA. The void and included volumes were determined using Blue dextran 2000 and bromophenol blue, respectively. After dissolving in buffer, myosins were clarified by centrifugation. Fractions of 27 drops (160 fractions total) were collected. The column was then equilibrated in high salt buffer (600 mM KCl, 5 mM $MgCl_2$, 1 mM EGTA, 10 mM K_nPO4, pH 7.5) and the procedure repeated. Proteins in low salt were detected by fluorescence, and in high salt by absorbance. The elution volumes of the IgG, IgM, BSA, Blue dextran 2000, and bromophenol blue did not change significantly with ionic strength. Thus, both labelled and unlabelled myosins exhibited phosphate-dependent folding and unfolding.

II analogue, and this measurement revealed a dose-dependent loss of fibres that correlated extremely well with dephosphorylation of myosin light chains (Kolega *et al.*, 1993). These observations are consistent with regulation of fibre assembly and contraction through myosin phosphorylation.

One area in which fluorescent analogues provide unique capabilities is in assessing spatial variations in the state of assembly and local concentration of cytoplasmic proteins. A striking example was provided when fluorescent actin and myosin analogues were co-injected into the same cell and the relative distribution of the two proteins followed during early stages of locomotion (DeBiasio *et al.*, 1988). To correct for subcellular differences in accessible volume and optical pathlength, actin and myosin II fluorescence were normalized to inert fluorescence volume indicators (dextran labelled with fluorescein). Newly formed cellular protrusions contained an elevated concentration of actin and very little or no myosin II. No well-defined structures were detected in the protrusions by fluorescence or video-enhanced contrast microscopy. Within 1–2 min, well-defined actin- and myosin II-containing structures were detected in the same protrusion, together with diffuse actin and myosin II. Thus, initial protrusive activity involved a local, relative increase in actin concentration, and did not appear to require structures containing myosin II.

The state of assembly of actin and myosin II in various regions of locomoting cells can be examined by a number of different approaches using fluorescent analogues. Fluorescence recovery after photobleaching (FRAP) is perhaps the most elegant of these. In this method, a laser is used to bleach a small region of the analogue in a cell, then the rate at which fluores-

Table 41.1 Myosin II and rhodamine-myosin II ATPase activity.

		Mg^{2+} *ATPase*	
	K-EDTA	−Actin	*+Actin*
Myosin	381	<0.1	0.4
Myosin-PO4	–	3.1	27
Rhodamine-myosin	372	0.3	0.5
Rhodamine-myosin-PO4	–	3.7	22

Activities were measured at 25°C using the procedure of Sellers *et al.* (1981). K-EDTA activity was measured in a mixture containing 500 mM KCl,1 mM ATP, 2 mM EDTA, 15 mM Tris-HCl, and 45–90 nM myosin, pH 7.5. MgATPase activity was measured in 30 mM KCl, 5 mM $MgCl_2$, 1 mM ATP, 0.1 mM EGTA, and 15 mM Tris, pH 7.5, using 540 nM myosin. For actin activation, actin was added at a concentration of 0.3 mg ml^{-1}. Myosins were phosphorylated using the procedure described in Fig. 41.3, except that ATP was replaced with adenosine 5′-O-(3-thiotriphosphate). ATP hydrolysis rates are given as nmol min^{-1} mg^{-1}.

cence is restored by diffusion of molecules from outside the photobleached spot is measured. In FRAP studies of locomoting fibroblasts, myosin II analogue had essentially no translational mobility in regions near the leading edge, in contrast to a 79% mobile fraction in the perinuclear region (DeBiasio *et al.*, 1988; Kolega & Taylor, 1991). Thus, myosin II was not readily available for diffusion into a protrusion even though it was present at the protrusion's base and in areas within the leading edge. Active transport may be required to mobilize myosin II into established protrusions, possibly by molecular interactions with actin in the protrusion. The increase in myosin II mobility in the perinuclear region is consistent with disassembly of myosin II, and a similar perinuclear increase in myosin II mobility was observed in serum-deprived fibroblasts, where fibres are continuously assembled at the cell periphery, transported centripetally, and disassembled in the perinuclear cytoplasm (Kolega & Taylor, 1991).

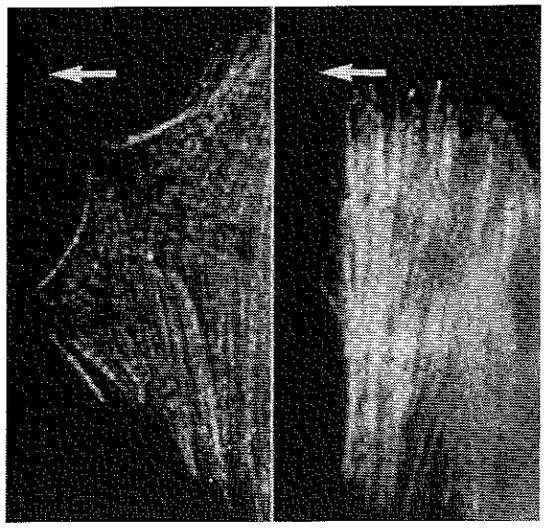

Figure 41.4 Fluorescent images of rhodamine-myosin II and rhodamine-myosin 20 kDa light chain analogues in Swiss 3T3 fibroblasts. Left: light chain analogue. Right: myosin II analogue. These cells are representative of a motile population 3–6 h after wounding. The arrows point in the direction of migration. Both analogues are distributed in a periodic, 'semisarcomeric' pattern.

FRAP measurements are restricted to a small number of small spots within any given cell. Much more extensive maps of assembly can be obtained by following the redistribution of an analogue when the cell is lysed with mild detergent. Freely diffusing material perfuses away from the cell, while material that is associated with structural elements remains in place. Comparison of pre- and post-permeabilization images reveals the proportion of bound material at any point in the cell. This approach has revealed a gradient in the assembly of myosin II across locomoting fribroblasts (Kolega & Taylor, 1993) and endothelial cells (Kolega, 1997). Myosin II was found to be extensively associated with the cytoskeleton at the base of the cells' leading protrusions, even when discrete fibrous structures were not apparent by fluorescence microscopy. Verkhovsky *et al.* (1995) followed the exact distribution of a myosin II analogue at high magnification to verify that the distribution of myosin II-containing structures was preserved during permeabilization and extensive post-permeabilization treatments. This allowed them to perform subsequent electron microscopic studies that have identified heretofore unknown forms of myosin II organization in non-muscle cells.

An additional trick allows one to infer the state of assembly of an analogue without permeabilizing (and stopping the movement of) cells. This entails comparing the distribution of the analogue with an inert, fluorescent tracer of the same size, which serves as an indicator of the volume that is accessible to the analogue. The extent to which the functional analogue becomes locally concentrated relative to the volume indicator can reveal when and where the analogue is binding or assembling in the cytoskeleton. Ratio images comparing the distribution of an assembly-competent analogue of myosin II with an assembly-incompetent counterpart confirmed the spatial variations in myosin II assembly revealed by FRAP and detergent-permeabilization (Kolega & Taylor, 1993). Actin assembly can be visualized in a similar fashion (Giuliano & Taylor, 1994). Thus, time-lapse, ratio imaging can produce dynamic maps of structural

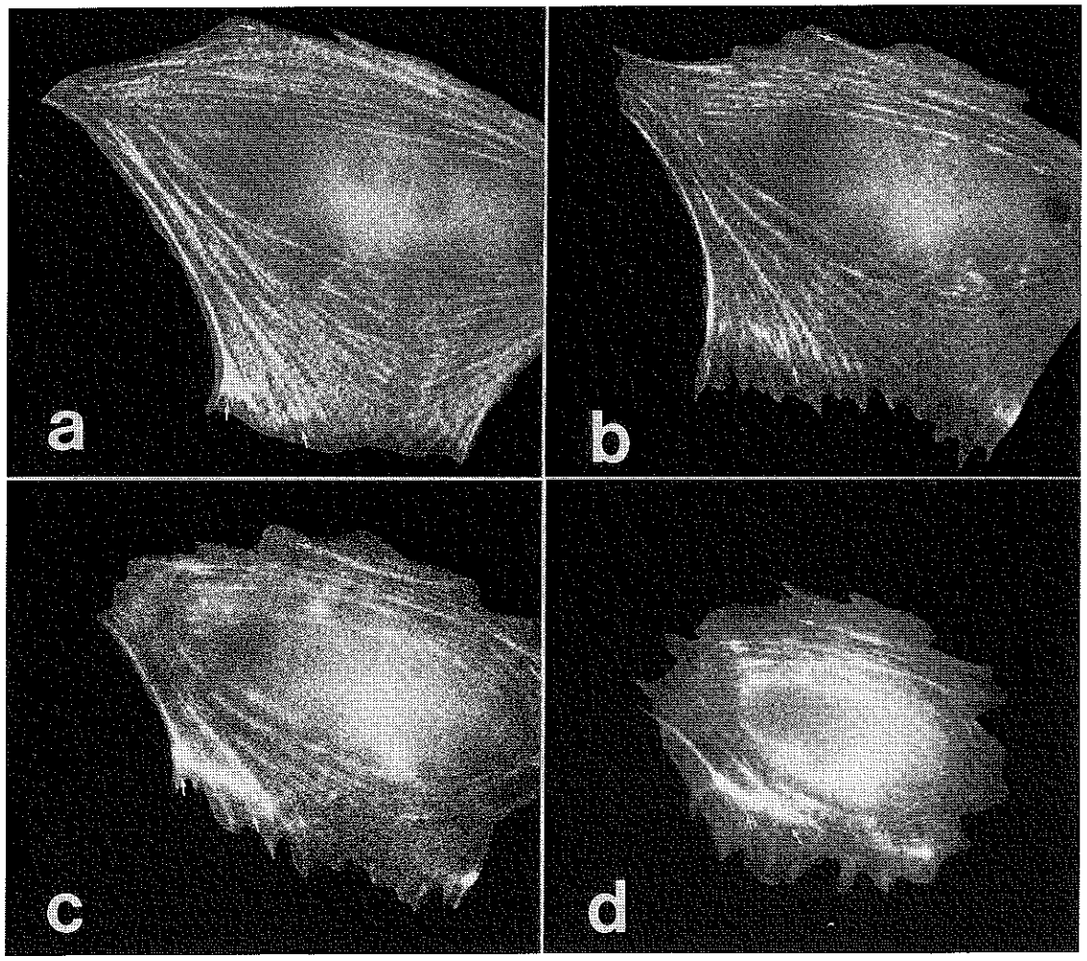

Figure 41.5 Myosin contraction in fibroblasts after treatment with phosphatase inhibitor. Quiescent, serum-deprived Swiss 3T3 fibroblasts were treated with a 400 nM solution of okadaic acid, a phosphatase inhibitor. Images were acquired with a cooled CCD camera at 2.5 min intervals. Small arrows identify selected myosin labelled fibres. (a) Myosin labelled fibres were distributed throughout the quiescent cell, displaying a relatively uniform punctuate distribution, (b) 25 min, (c) 40 min, (d) 55 min after okadaic treatment. Myosin-labelled fibres contracted from the cell periphery towards the mucleus over time. The cell edges detached from the substrate and retracted.

components as they assemble and disassemble in living cells.

Understanding how different myosin motors move within living cells should greatly facilitate our understanding of the mechanisms of cell locomotion. This is particularly true as we attempt to unravel the functions of myosin II and the ever-growing family of unconventional myosins (for reviews, see Mooseker & Cheney, 1995; Sellers *et al.*, 1996). The use of fluorescent analogue cytochemistry in this effort has recently been revolutionized by the cloning of green fluorescent protein (GFP). The portion of the GFP molecule that is required for fluorescence can now be engineered into proteins to give them an integral fluorescent tag. While the large size of the fluorescent GFP piece (20–30 kDa) can potentially disrupt a protein's normal function, if carefully engineered and tested, GFP-analogues can be extremely powerful tools. A GFP-myosin fusion protein has been shown to maintain its ATPase activity (Iwane *et al.*, 1997), and a GFP sequence has been spliced into the heavy chain of myosin II in *Dictyostelium* (Moores *et al.*, 1996), creating an organism in which endogenous myosin II can be monitored by fluorescence microscopy, in any cell at any time, and without microinjection. These new tools, in conjunction with the existing analogues of myosin II and other cytoskeletal proteins, continue to expand our window onto the workings of the cell's locomotive machinery.

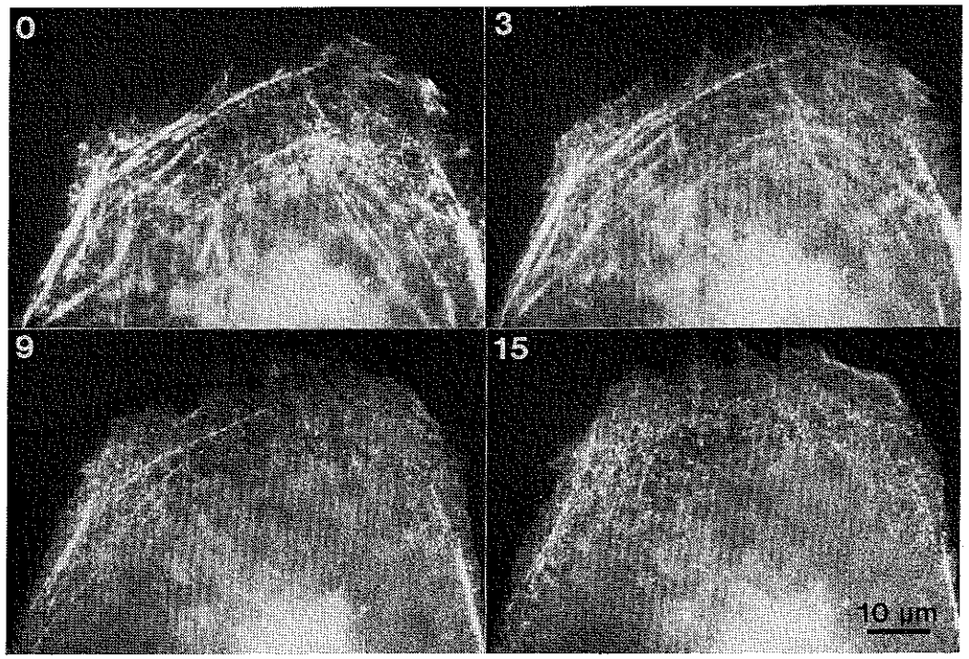

Figure 41.6 Dissolution of stress fibres in the presence of kinase inhibitor. Serum-deprived Swiss 3T3 fibroblasts were microinjected with a rhodamine analogue of myosin II. After 60 min. during which the analogue became distributed through the cytoplasm, the cell was perfused with 50 μM staurosporine while fluorescence images were acquired at 1 min intervals using a cooled CCD camera. Selected images from the sequence are shown with the time in minutes after perfusion indicated in the upper left. Prior to treatment, myosin II was located predominantly in stress fibres. Upon perfusion of inhibitor, stress fibres appeared to dissolve: fluorescence decreased uniformly along the length of the fibres while diffuse cytoplasmic fluorescence increased until little or no fibre structure remained.

41.4 PROTEIN-BASED OPTICAL BIOSENSORS OF MYOSIN II REGULATORY LIGHT CHAIN PHOSPHORYLATION

Smooth muscle and non-muscle cells express a myosin II molecule consisting of a pair of heavy chains that form two globular head domains (which contain the actin- and ATP-binding sites), a neck domain (containing the light chain binding sites), and a coiled-coil tail domain. Non-covalently associated with the neck are two pairs of light chains – the essential light chains and the regulatory light chains. The regulatory light chains undergo covalent, reversible phosphorylation, which helps to regulate the activity of the myosin motor domain (reviewed by Sellers & Adelstein, 1987; Moussavi *et al.*, 1993; Sellers & Goodson, 1995). Serine-19, or analogous serine (and sometimes threonine-18), of the regulatory light chain is phosphorylated by the calcium/calmodulin-dependent enzyme myosin light chain kinase. *In vitro*, phosphorylation at this site exhibits several effects on the entire myosin-II molecule: the actin-activated MgATPase activity is increased by several hundred-fold; the protein shifts from a 10S unphosphorylated, folded conformation to a 6S, phosphorylated extended conformation; and the phosphorylated 6S particle assembles into bipolar thick filaments. In addition, serine-1, serine-2 and threonine-9 of the regulatory light chain can be phosphorylated by phospholipid-dependent protein kinase C and cyclin-p34^{cdc2}. Phosphorylation at these 'inhibitory' sites decreases the actin-activated MgATPase activity of myosin II previously phosphorylated on serine-19 (by myosin light chain kinase), but has little effect on the actin-activated MgATPase of myosin II previously *un*phosphorylated on serine-19. Additionally, phosphorylation of serine-1, serine-2 and threonine-9 decreases the affinity of myosin light chain kinase for the regulatory light chain.

Cellular effects of myosin-II phosphorylation have previously been studied using dilute solution biochemistry or extracted cell models. Recently, phosphorylation-specific myosin-II regulatory light chain antibodies have been used in fixed cells to study regulatory light chain phosphorylation in time and space (Bennett *et al.*, 1988; Matsumura *et al.*, 1998). These measurements of the phosphorylation state of cell

populations have provided valuable information about the regulatory role of this event *in vivo*, but these methods can only report the cell population average. Our laboratory has designed novel, phosphorylation-sensitive fluorescent derivatives of myosin II, with the aim of learning more about how the temporal and spatial regulation of myosin II contributes to non-muscle cell motility in individual, living cells. This section describes the design of two fluorescent protein biosensors of myosin II that report myosin II activity *in situ* or *in vivo*. One reagent was used in locomoting and dividing cells to help understand the contribution of myosin II to these events.

Before we produced a phosphorylation-sensitive light chain analogue, it was important to establish that light chains could be fluorescently labelled in such a way that they would retain nearly native biochemical activity and would incorporate into the myosin II of living cells. Model studies were carried out using a turkey gizzard light chain labelled with an environmentally insensitive dye, tetramethylrhodamine-5,(6)iodoacetamide. This analogue could be fully phosphorylated *in vitro* with myosin light chain kinase isolated from smooth muscle; the rate of phosphorylation was 70% that of unlabelled myosin II. When injected into live cells, the analogue exchanged with native myosin II regulatory light chains and incorporated into actin/myosin-based fibres in both non-motile and actively migrating cells. The analogue showed the same punctate, periodic fluorescence pattern that we have observed with the whole myosin II analogue (Fig. 41.4). Similar results have been obtained with light chains from striated muscle (Mittal *et al.*, 1987). This *in vivo* exchange provides a versatile method for the introduction of light chains into myosin II within live cells. Biochemical studies have shown that regulatory light chains are functionally interchangeable among species.

We have designed two phosphorylation-sensitive fluorescent biosensors using two different approaches. Via a molecular genetic approach, a regulatory light chain was engineered to contain a single cysteine (residue 18) adjacent to the phosphorylated serine (residue 19) (Post *et al.*, 1994). This regulatory light chain was labelled with the polarity-sensitive fluorescent dye acrylodan on the newly inserted cysteine. Phosphorylation of this labelled light chain (called AC-cys18·LC_{20}) by MLCK produces a 60% quenching and a 28 nm red shift of fluorescence emission. The labelled, mutant light chain was reconstituted with smooth muscle myosin II heavy chains and essential light chains with an *in vitro* light chain exchange procedure of Katoh & Lowey (1989). Biochemical assays demonstrated that this phosphorylation biosensor retains nearly native levels of rate of phosphorylation, K^+ATPase activity, and *in vitro* motility. The acrylodan-labelled mutant light chain was exchanged into the A-bands of chicken pectoralis myofibrils *in situ* to demonstrate the localization and activity of the biosensor in a highly ordered contractile system. Fluorometry and quantitative fluorescence microscopic imaging experiments demonstrated a phosphorylation-dependent fluorescence change in AC-cys18·LC_{20} exchanged myofibrils. Labelled mutant light chains were also incorporated into stress fibres of living fibroblasts and smooth muscle cells. This reagent has been valuable for *in vitro* and *in situ* studies, but severe intracellular quenching has limited its usefulness for live cell studies.

The second approach employs fluorescence resonance energy transfer between fluorescein-labelled regulatory light chains to rhodamine-labelled essential light chains and heavy chains (Post *et al.*, 1995). Native regulatory light chains were labelled at their single cysteine (cys 108) with fluorescein; these labelled light chains were incorporated into the rhodamine-labelled myosin II analogue (see Section 47.3). The ratio of rhodamine/fluorescein emission increases by up to 26% with regulatory light chain phosphorylation by myosin light chain kinase. The majority of the change in energy transfer is from regulatory light chain phosphorylation by myosin light chain kinase (versus phosphorylation by protein kinase C). Myosin II folding/unfolding, filament assembly, and actin-binding do not significantly affect the energy transfer ratio of this biosensor. Treatment of fibroblasts containing the phosphorylation biosensor with the kinase inhibitor staurosporine produced a lower ratio of rhodamine/fluorescein emission. This corresponds to a lower level of myosin II regulatory light chain phosphorylation and correlates with previously obtained biochemical measurements of the state of phosphorylation in these cells (Giuliano *et al.*, 1992). This biosensor has been microinjected into living cells, where it incorporates into stress fibres. Locomoting fibroblasts containing the biosensor showed a gradient of myosin II phosphorylation that was lowest near the leading edge and highest in the tail region of these cells, which correlates with previously observed gradients of free calcium and activated calmodulin (Plate 47.1) (Brundage *et al.*, 1991; Hahn *et al.*, 1992; Gough & Taylor, 1993). Note that while phosphorylation is highest in the rear of the cell, myosin II concentration is low and actin and myosin II filament assembly is low (Kolega & Taylor, 1993; Guiliano & Taylor, 1994; Post *et al.*, 1995). This suggests that, in the tail region, where myosin II is maximally activated, a solation of the actin-myosin gel occurs to allow for maximum contractility of the activated myosin II motor (Janson & Taylor, 1993).

Fibroblasts (microinjected with this biosensor)

undergoing cell division showed a global increase in serine 19 myosin II regulatory light chain phosphorylation at anaphase onset. The level of phosphorylation remained elevated throughout telophase and into cytokinesis near the equatorial region, while regulatory light chain phosphorylation decreased at the polar regions, creating a bipolar dividing cell (DeBiasio *et al.*, 1996). At the same time, myosin II-based fibres shortened in the cleavage furrow. Elevated levels of phosphorylated myosin II correlated well with elevated concentrations of myosin II in the cleavage furrow (DeBiasio *et al.*, 1996). These results suggest a contractile force at the cell equator may be generated, at least in part, through activation of myosin II (via phosphorylation of serine 19 of the regulatory light chain) at the cleavage furrow in conjunction with deactivation of myosin II at the polar regions.

Future myosin II biosensors will combine both the genetic and the energy transfer approaches. Genetic engineering will be used to move labelling sites to maximize detection of a conformational change. We have demonstrated the feasibility of these approaches and have provided previously unobtainable information about the state of myosin II regulatory light chain phosphorylation in individual, living motile cells.

41.5 FUTURE STUDIES

Recent developments in design of protein-based indicators hold promise for the observation of a wide range of protein activities *in vivo*, including protein conformational changes, post-translational modification, and ligand binding. Proteins have evolved to recognize physiologically relevant molecules with great specificity, and can be modified to become fluorescent indicators of small molecule concentration. Production of protein-based indicators is currently being pursued through two routes, using environmentally sensitive dyes or fluorescence energy transfer. These approaches have complementary strengths and shortcomings which will determine their applicability in particular situations. Genetic engineering of analogues will be a key tool, enabling precise positioning of attached fluorophores.

The ability to use a single environmentally sensitive fluorophore, rather than the two dyes required for energy transfer, will have obvious advantages in some situations. Maintenance of biological activity in a small protein (such as calmodulin) will be much more difficult after attachment of two dyes. Site-specific attachment of even a single dye is difficult. Intact biological activity will be important in indicators where biological regulation of ligand affinity is being studied, as in indicators revealing the regulation of signalling proteins.

When a protein is modified to become an indicator of small molecule concentration, intact biological activity may, in fact, be undesirable. The indicator should strictly reflect the concentration and distribution of the target ligand. The indicator's distribution and target affinity should not be affected by binding of other ligands, post-translational modification, or other regulatory effects. In such cases, energy transfer would be more applicable because disruption of certain protein activities will be desirable. The primary obstacle to designing useful indicators of small signalling molecules is the unavoidable buffering of these molecules by the indicator itself. Buffering must be minimized by loading very small quantities of indicator. This will require development of bright fluorescent proteins which show strong fluorescence changes when binding their targets. Access to practical small molecule indicators may ultimately depend on the development of very bright dyes suitable for use in living cells.

Indicators of protein–protein binding may be more accessible using currently available methodology. The high concentrations of some intracellular proteins permit loading of relatively large indicator concentrations. Indicators of protein-protein binding could be made by modifying one of the two interacting proteins. Either solvent-sensitive dyes or energy transfer pairs could be used to indicate a protein conformational change induced specifically by the targeted ligand. It may be possible to make indicators with great specificity for a single protein-protein interaction by placing a different dye on each of the interacting proteins, and monitoring energy transfer as an indicator of protein binding. This approach will likely require covalent attachment of the two proteins via a flexible tether. Without such a tether, the labelled proteins could bind to unlabelled, endogenous proteins rather than to each other, necessitating the loading of unacceptably large indicator concentrations to produce detectable energy transfer.

Both energy transfer dyes and environmentally sensitive fluorophores may potentially interact with cellular components to produce artifactual fluorescence changes. Solvent-sensitive fluorophores can interact with lipids and hydrophobic proteins, and energy transfer will be sensitive to microviscosity and factors influencing dye orientation. Environmentally sensitive dyes can be designed with a strong affinity for the tagged protein to avoid artifactual binding to intracellular components. Meaningful interpretation of indicator data will require careful standardization of fluorescence response, both *in vitro* and when possible *in vivo*. Fluorescent calcium indicators have been calibrated within living cells using calcium ionophores

and external calcium buffers to control intracellular calcium (Spurgeon *et al.*, 1990).

Intracellular indicators of protein activity promise to yield otherwise inaccessible information about transient protein activity and its regulation in individual, living cells. The cell-to-cell heterogeneity observed in calcium signalling studies suggests that observation of single cells will be critical in untangling the complex interactions of signalling proteins (Byron & Villereal, 1989; Tucker & Fay, 1990). In this and other areas, fluorescent protein indicators should elucidate protein function *in vivo*, thus enabling integration of biochemical data into models of global function. The regulation of many proteins has to date been approachable only through observation of interactions with isolated cellular components. It may soon be possible to observe proteins regulated by the full complement of cellular controls, including those not yet characterized or even postulated.

The most exciting experiments will combine multiple reagents in the same cell or tissue to permit correlations between various parameters in time and space. Ultimately, we would like to monitor changes in free calcium, calcium binding to calmodulin, phosphorylation of myosin II regulatory light chains and myosin II dynamics in the same experiment. Therefore, the optimal combination of reagents and instrumentation continues to be a great opportunity and challenge.

REFERENCES

Adams S.R., Harootunian A.T., Buechler Y.J., Taylor S.S. & Tsien R.Y. (1991) *Nature* **349**, 694–697.

Andreason T.J., Luetje C.W., Heideman W. & Storm D.R. (1983) *Biochemistry* **22**, 4615–4618.

Bennett J.P., Cross R.A., Kendrick-Jones J. & Weeds A.G. (1988) *J. Cell Biol.* **107**, 2623–2629.

Bright G.R., Fisher G.W., Rogowska J. & Taylor D.L. (1989) *Methods Cell Biol.* **30**, 157–190.

Brundage R.A., Fogarty K.E., Tuft R.A. & Fay F.S. (1991) *Science* **254**, 703–706.

Byron K.L. & Villereal M.L. (1989) *J. Biol. Chem.* **264**, 18234–18239.

Chandra T.S., Nath N., Suzuki H. & Seidel J.C. (1985) *J. Biol. Chem.* **260**, 202–207.

Cohen P. & Klee C. (eds) (1988) *Calmodulin*. Elsevier, New York.

Comte M., Maulet Y. & Cox J. (1983) *Biochem. J* **209**, 269–272.

Cox J.A., Comte M., Fitton J.E. & DeGrado W.F. (1985) *J. Biol. Chem.* **260**, 2527–2534.

DeBiasio R.L., Wang L., Fisher G.W. & Taylor D.L. (1988) *J. Cell Biol.* **107**, 2631–2645.

DeBiasio R.L., LaRocca G.M., Post P.L. & Taylor, D.L. (1996) *Mol. Biol. Cell* **7**, 1259–1282.

Fisher G.W., Conrad P.A., DeBiasio R.L. & Taylor D.L. (1988) *Cell Motil. Cytoskeleton* **11**, 235–247.

Guilano K.A., Kolega J., DeBiasio R.L. & Taylor D.L. (1992) *Molec. Biol. Cell* **3**, 1037–1048.

Giuliano K.A. & Taylor D.L. (1990) *Cell Motil. Cytoskeleton* **16**, 14–21.

Giuliano K.A. & Taylor D.L. (1994) *J. Cell Biol.* **124**, 971–983.

Giuliano K.A., Nederlof M.A., DeBiasio R., Lanni F., Waggoner A.S. & Taylor D.L. (1990) In *Optical Microscopy for Biology* (Herman B. & Jacobson K. eds). Wiley-Liss, New York, pp. 537–543.

Gorbsky G.J., Sammak P.J. & Borisy G.G. (1987) *J. Cell Biol.* **104**, 9–18.

Gough A.H. & Taylor D.L. (1993) *J. Cell Biol.* **121**, 1095–1107.

Hahn K.M., Waggoner A.W. & Taylor D.L. (1990) *J. Biol. Chem.* **265**, 20335–20345.

Hahn K., DeBiasio R.L. & Taylor, D.L. (1992) *Nature* **359**, 736–738.

Iwane A.H., Funatsu T., Harada Y., Tokunaga M., Ohara O., Morimoto S. & Yanagida T. (1997) *FEBS Lett* **407**, 235–238.

Janson L.W. & Taylor D.L. (1993) *J. Cell Biol.* **123**, 345–356.

Katoh T., & Lowey S. (1989) *J. Cell Biol.* **109**, 1549–1560.

Klee C.B. (1988) In *Calmodulin*, P. Cohen & C. Klee (eds). Elsevier, New York, pp. 35–53.

Kolega J. (1997) *Exp. Cell Res.* **231**, 66–82.

Kolega J. (1988) *J. Cell. Biochem.* **68**, 389–401.

Kolega J. & Taylor D.L. (1991) *Curr. Topics Membr.* **38**, 187–206.

Kolega J. & Taylor D.L. (1993) *Molec. Biol. Cell* **4**, 819–836.

Kolega J., Janson L.W. & Taylor D.L. (1991) *J. Cell Biol.* **114**, 993–1003.

Kolega J., Nederlof M.A. & Taylor D.L. (1993) *Bioimaging* **1**, 136–150.

Kreis, T.E. & Birchmeier W. (1982) *Int. Rev. Cytol.* **75**, 209–227.

Lamb, N.J.C., Fernandez A., Conti M.A., Adelstein R., Glass D.B., Welch W.J. & Feramisco J.R. (1988) *J. Biol. Chem.* **106**, 1955–1971.

LaPorte D.C., Wierman B.M. & Storm D.R. (1980) *Biochemistry* **19**, 3814–3819.

LaPorte D.C., Keller C.H., Olwin B.B. & Storm D.R. (1981) *Biochemistry* **20**, 3965–3972.

Luby-Phelps K., Lanni F., Taylor D.L. (1985) *J. Cell Biol.* **101**, 1245–1256.

McKenna N.M., Wang Y.-l. & Konkel M.E. (1989) *J. Cell Biol.* **109**, 1163–1172.

McNeil P.L. & Taylor D.L. (1987) *Cell Membranes*, vol. 3 (Elson E., Frazier W. & Glaser L., eds) Plenum Publishing, New York, 365–405.

McNeil P.L., McKenna M.P. & Taylor D.L. (1985) *J. Cell Biol.* **101**, 372–379.

Malencik D.A., Anderson S.R., Shalitin Y. & Schimerlik M.I. (1981) *Biochem. Biophys. Res. Commun.* **101**, 390–395.

Manalan A.S. & Klee C.B. (1984) *Adv. Cyclic Nucleotide Protein Phosphorylation Res.* **18**, 227–277.

Matsumura F., Ono S., Yamakita Y., Totsukawa G. & Yamashiro S. (1998) *J. Cell Biol.* **140**, 119–129.

Maulet Y. & Cox J.A. (1983) *Biochemistry* **22**, 5680–5686.

Mills J.S., Walsh M.P., Nemcek K. & Johnson J.D. (1988) *Biochemistry* **27**, 991–996.

Mitchison T.J. (1989) *J. Cell Biol.* **109**, 637–652.

Mittal B., Sanger J.M. & Sanger J.W. (1987) *J. Cell Biol.* **105**, 1753–1760.

Moores S.L., Sabry J.H. & Spudich J.A. (1996) *Proc. Natl Acad. Sci. USA* **93**, 443–446.

Mooseker M.S. & Cheney R.E. (1995) *Annu. Rev. Cell Devel. Biol,* **11**, 633–675.

Moussavi R.S., Kelley C.A. & Adelstein R.S. (1993) *Mol. Cell. Biochem.* **127**, 219–227.

Nath N., Nag S. & Seidel J.C. (1986) *Biochemistry* **25**, 6169–6176.
Pardue R.L., Kaetzel M.A., Hahn S.H., Brinkley B.R. & Dedman J.R. (1981) *Cell* **23**, 533–542.
Perrie W.T. & Perry S.V. (1970) *Biochem. J.* **119**, 31–38.
Post P.L., Trybus K.M. & Taylor D.L. (1994) *J. Biol. Chem.* **269**, 12 880–12 887.
Post P.L., DeBiasio R.L. & Taylor D.L. (1995) *Mol. Biol. Cell* **6**, 1755–1768.
Salmon E.D., Leslie R.J., Saxton W.M., Karow M.L. & McIntosh J.R. (1984) *J. Cell Biol.*, **99**, 2165–2174.
Sanger J.M., Mittal B., Dome J.S. & Sanger J.W. (1989) *Cell Motility Cytoskeleton* **14**, 201–219.
Seeholzer S.H., Cohn M., Putkey J.A., Means A.R. & Crespi H.L. (1986) *Proc. Natl Acad. Sci. USA* **83**, 3634–3683.
Sellers J.R. & Adelstein R.S. (1987) In *The Enzymes* (Boyer P.D. ed.). Academic Press, Orlando, pp. 381–418.
Sellers J.R. & Goodson H.V. (1995) *Prot. Profile* **2**, 1323–1423.
Sellers J.R., Pato M.D. & Adlestein R.S. (1981) *J. Biol. Chem.* **256**, 13137–13142.
Sellers J.R., Goodson H.V. & Wang F. (1996) *J. Muscle Res. Cell Motility* **17**, 7–22.
Simon J.R. & Taylor D.L. (1986) *Methods Enzymol.* **134**, 487–507.
Spurgeon H.A., Stern M.D., Baartz G., Raffaeli S., Hausford R.G., Talo A., Lakatta E.G. & Capogrossi M.C. (1990) *Am. J. Physiol.* **258**, H574–H586.
Takuwa N., Iwamoto A., Kumada M., Yamashita K. & Takuwa Y. (1991) *J. Biol. Chem.* **266**, 1403–1409.
Tanasugarn L., McNeil P., Reynolds G.T. & Taylor D.L. (1984) *J. Cell Biol.* **98**, 717–724.
Taylor D.L. & Fechheimer M. (1982) *Phil. Trans. Roy. Soc. Lond. B* **299**, 185–197.
Taylor D.L. & Wang Y. (1978) *Proc. Natl Acad. Sci. USA* **75**, 857–861.
Taylor D.L. & Wang Y. (1980) *Nature* **284**, 405–410.
Taylor D.L., Reidler J., Spudich J.A. & Stryer L. (1981) *J. Cell Biol.* **89**, 362–367.
Taylor D.L., Amato P.A., Luby-Phelps K. & McNeil P.L. (1984) *Trends Biochem. Sci.* **9**, 88–91.
Theriot J.A. & Mitchison T.J. (1991) *Nature* **352**, 126–131.
Trybus K.M., Huiatt T.W. & Lowey S. (1982) *Proc. Natl Acad. Sci. USA* **79**, 6151–6155.
Tsien R.Y. (1989) *Methods Cell Biol.* **30**, 127–153.
Tucker R.W. & Fay F.S. (1990) *Eur. J. Cell Biol.* **51**, 120–127.
Vekhovsky A.B., Svitkina T.M. & Borisy G.G. (1995) *J. Cell Biol.* **131**, 989–1002.
Wadsworth P. & Salmon E.D. (1986) *J. Cell Biol.* **102**, 1032–1038.
Wang Y. (1989) *Methods Cell Biol.* **29**, 1–12.
Wang Y. & Taylor D.L. (1980) *J. Histochem. Cytochem.* **28**, 1198–1206.
Wang Y. Taylor D.L. (1981) *Cell* **27**, 429–436.
Wang Y., Heiple J.M. & Taylor D.L. (1982) *Methods Cell Biol.* **24B**, 1–11.
Ware B., Brvenik L.J., Cummings R.T., Furukawa R.H. & Krafft G.A. (1986) In *Applications of Fluorescence in the Biomedical Sciences*, D.L. Taylor, A.S. Waggoner, R.F. Murphy, F. Lanni & B.R. Birge (eds). Alan R. Liss, New York, pp. 141–157.
Zavortnik M., Welsh M.J. & McIntosh J.R. (1983) *Exp. Cell Res.* **149**, 375–385.